Journal of Sound and Vibration (1997) **203**(2), 181–192

FREE VIBRATION OF PARTIALLY CLAMPED RECTANGULAR PLATES WITH AND WITHOUT RIGID POINT SUPPORTS

R. K. SINGHAL

David Florida Laboratory, Canadian Space Agency, Ottawa, Ontario K2H 8S2, Canada

AND

D. J. GORMAN

Department of Mechanical Engineering, University of Ottawa, Ottawa, Ontario K1N 6N5, Canada

(*Received* 20 *March* 1996, *and in final form* 11 *November* 1996)

An analytical procedure based on the method of superposition is described for obtaining the free vibration frequencies and mode shapes of partially clamped cantilevered rectangular plates with and without rigid point supports. The supports are of the type provided by bolts with stand-offs. Good agreement is obtained when computed results are compared with those obtained experimentally. While the solution to this problem is of general interest it is of particular interest to people working in the design of electronic circuit boards.

© 1997 Academic Press Limited

1. INTRODUCTION

It is well known that the subject of free vibration analysis of rectangular plates with mixed boundary conditions is one that has received little attention over the years. By "mixed boundary conditions" one refers to situations where there are discontinuities in the type of support supplied to one or more of the plate edges. A typical example of such edge support, and one that is encountered here, involves a plate with clamping part way along an edge, the remainder of the edge being free.

In this paper one begins by examining the free vibration frequencies and mode shapes of a thin rectangular plate with three entirely free edges, the remaining edge being clamped continuously throughout a region beginning at one corner and extending part way along the boundary. The remainder of this edge is free support. It is for this reason such a plate is referred to as a "partially clamped cantilever plate".

Plates with this type of edge support are sometimes employed as electronic circuit boards in the electronic industry. It is also known that such plates are sometimes given further lateral support by means of what are referred to as "bolts and stand-offs". This lateral support is usually supplied by a bolt which on one end is attached to a rigid base. The bolt also passes through the thin plate and by means of a threaded nut and hollow cylindrical spacer imparts rigid support to the plate in the immediate region. Such support is referred to herein as "rigid point support". The principal objective of this paper is to demonstrate how accurate analytical type solutions can be obtained for the partially clamped plate both with, and without additional point support from bolts and standoffs.

0022–460X/97/220181 + 12 $25.00/0/sv960878 © 1997 Academic Press Limited

A number of experimental tests have been conducted in order to permit comparison between theory and experiment. It will be obvious that the fundamental and other frequencies of such plates will be highly dependent on the location of the bolt-standoff supports.

2. ANALYTICAL PROCEDURE

2.1. DEVELOPMENT OF BUILDING BLOCK SOLUTIONS

Two steps are to be accomplished in the analytical procedure. The first is to obtain a solution for the partially clamped plate. The second step involves incorporating the effects of rigid point supports on the plate behaviour.

An analytical type solution is obtained for the entire problem by superimposing a set of judiciously chosen rectangular plate forced vibration solutions. Unknown coefficients appearing in the superimposed set are constrained in such a manner that all of the prescribed boundary conditions are satisfied. Prescribed displacement conditions in the region of the rigid body support are also satisfied. In the study described here only one rigid point support is considered to act. It will be seen that incorporating the effects of additional point supports is easily taken care of. One wishes to prepare a general analysis capable of handling the plate problem shown schematically in Figure 1.

Consider the nine rectangular plate forced vibration problems (building blocks) of Figure 2. Only the solution for the first building block will be provided in detail. All of the non-driven edges of the building blocks are given slip–shear support, indicated by two small circles adjacent to the edges. Along such edges vertical edge reaction, and slope taken normal to the edge, are everywhere zero.

The driven edge, $\eta = 1$, of the first building block is free of bending moment. To begin, one considers this edge to be driven by a concentrated harmonic lateral force of circular frequency ω located a dimensionless distance ζ along the edge. The dimensionless amplitude of this driving force is represented by a Dirac delta function as indicated in the figure. This function is expanded in a cosine series as

$$\frac{V(\xi)b^3}{aD} = \sum_{m=0,1}^{k} \frac{2V_0}{\delta_m} \cos m\pi\zeta \cos m\pi\xi, \tag{1}$$

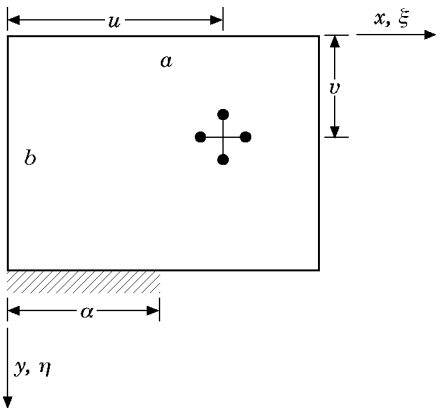

Figure 1. Partially clamped cantilever plate with bolt and stand-off.

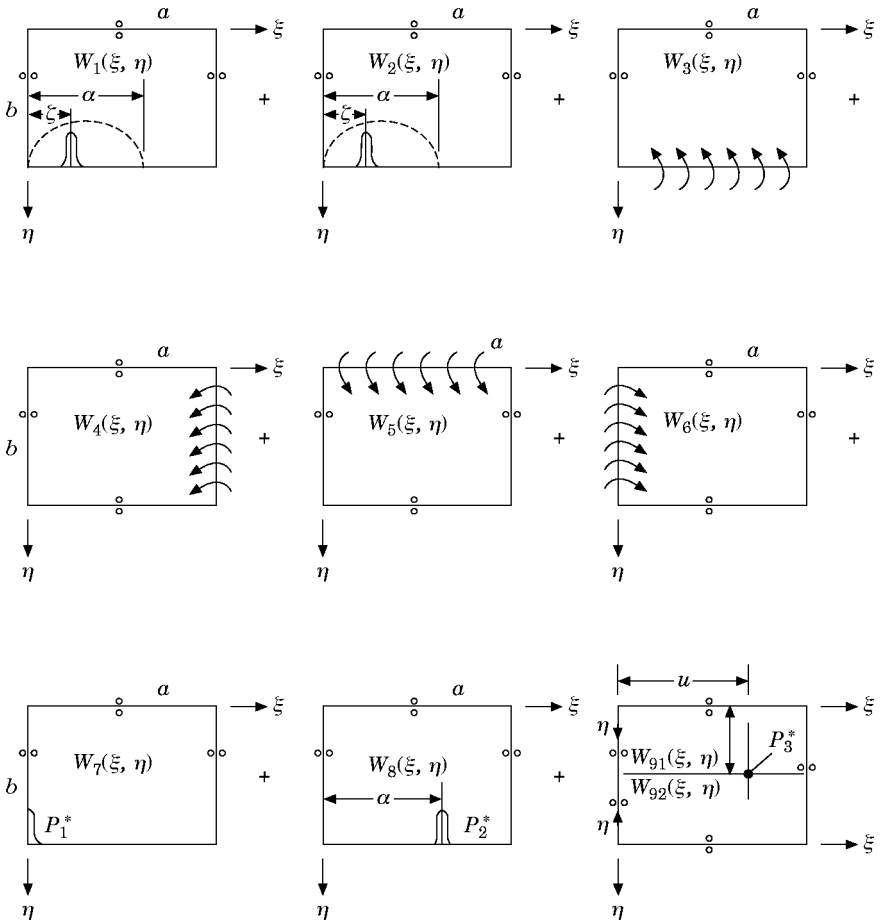

Figure 2. Nine building blocks utilized in analysing partially clamped rectangular plates with single point support.

where $\delta_m = 2$, for $m = 0$; $\delta_m = 1$, for $m \neq 0$, and V_0 is the dimensionless harmonic force amplitude.

The response of the plate to this driving force can be expressed in the form proposed by Lévy as

$$W(\xi, \eta) = \sum_{m=0,1}^{k} Y_m(\eta) \cos m\pi\xi. \tag{2}$$

Upon substituting Equation (2) into the governing differential equation it is found that $Y_m(\eta)$ may be expressed as, for $\lambda^2 > (m\pi)^2$,

$$Y_m(\eta) = A_m \cosh \beta_m\eta + B_m \sinh \beta_m\eta + C_m \cos \gamma_m\eta + D_m \sin \gamma_m\eta. \tag{3}$$

And, for $\lambda^2 < (m\pi)^2$,

$$Y_m(\eta) = A_m \cosh \beta_m\eta + B_m \sinh \beta_m\eta + C_m \cosh \gamma_m\eta + D_m \sin \gamma_m\eta, \tag{4}$$

where A_m, B_m, etc., are constants to be determined, $B_m = \phi\sqrt{\lambda^2 + (m\pi)^2}$, $\gamma_m = \phi\sqrt{\lambda^2 - (m\pi)^2}$ or $\phi\sqrt{(m\pi)^2 - \lambda^2}$, whichever is real. The vertical edge reaction can

also be written as

$$\frac{V(\xi)b^3}{aD} = -\left[\frac{\partial^3 W(\xi,\eta)}{\partial n^3} + v^*\phi^2 \frac{\partial^3 W(\xi,\eta)}{\partial\eta\partial\xi^2}\right]_{\eta=1}. \tag{5}$$

Enforcing the set of four boundary conditions, including the equality of the right hand sides of equations (1) and (5), we readily obtain, for $\lambda^2 > (m\pi)^2$,

$$Y_m(\eta) = A_m[\cosh\beta_m\eta + \theta_{1m}\cos\gamma_m\eta] \tag{6}$$

with

$$A_m = (-2V_0/\delta_m)(\cos m\pi\zeta/\theta_{11m}). \tag{7}$$

And, for $\lambda^2 < (m\pi)^2$,

$$Y_m(\eta) = A_m[\cosh\beta_m\eta + \theta_{2m}\cosh\gamma_m\eta], \tag{8}$$

where

$$A_m = (-2V_0/\delta_m)(\cos m\pi\zeta/\theta_{22m}), \tag{9}$$

$$\theta_{1m} = \frac{[\beta_m^2 - v\phi^2(m\pi)^2]\cosh\beta_m}{[\gamma_m^2 + v\phi^2(m\pi)^2]\cos\gamma_m}, \qquad \theta_{2m} = \frac{-[\beta_m^2 - v\phi^2(m\pi)^2]\cosh\beta_m}{[\gamma_m^2 - v\phi^2(m\pi)^2]\cosh\gamma_m}, \tag{10, 11}$$

$$\theta_{11m} = \beta_m[\beta_m^2 - v^*\phi^2(m\pi)^2]\sinh\beta_m + \theta_{1m}\gamma_m[\gamma_m^2 - v^*\phi^2(m\pi)^2]\sin\gamma_m \tag{12}$$

and

$$\theta_{22m} = \beta_m[\beta_m^2 - v^*\phi^2(m\pi)^2]\sinh\beta_m + \theta_{2m}\gamma_m[\gamma_m^2 - v^*\phi^2(m\pi)^2]\sinh\gamma_m. \tag{13}$$

Achievement of the above solution constitutes an intermediate step in obtaining a solution for the first building block.

Let the total edge reaction along the driven edge of the first building block, in the interval $0 \leqslant \xi \leqslant \alpha$, be expanded in series form as

$$\frac{V(\xi)b^3}{aD} = \sum_{j=0,1}^{k_L} E_j \cos\frac{j\pi\zeta}{\alpha}. \tag{14}$$

Beyond this region, ($\xi > \alpha$), edge reaction is zero.

The distributed reaction is represented schematically by the broken line in the figure. Then, utilizing the process of integration to obtain the resultant values for the quantities, A_m, of equations (7) and (9), one has, for $\lambda^2 > (m\pi)^2$,

$$A_m = \frac{-2}{\delta_m}\sum_{j=0,1}^{k_L}\frac{E_j}{\theta_{11m}}\int_0^\alpha \cos\frac{j\pi\zeta}{\alpha}\cos m\pi\zeta\ \mathrm{d}\zeta \tag{15}$$

and, for $\lambda^2 < (m\pi)^2$,

$$A_m = \frac{-2}{\delta_m}\sum_{j=0,1}^{k_L}\frac{E_j}{\theta_{22m}}\int_0^\alpha \cos\frac{j\pi\zeta}{\alpha}\cos m\pi\zeta\ \mathrm{d}\zeta. \tag{16}$$

Introducing the symbol ϕ_{jm}, where

$$\phi_{jm} = \int_0^{\alpha} \cos\frac{j\pi\zeta}{\alpha} \cos m\pi\zeta \, \mathrm{d}\zeta, \tag{17}$$

equations (15) and (16) may be written as

$$A_m = \frac{-2}{\delta_m} \sum_{j=0,1}^{\infty} \frac{E_j}{\theta_{11m}} \phi_{jm}, \qquad A_m = \frac{-2}{\delta_m} \sum_{j=0,1}^{\infty} \frac{E_j}{\theta_{22m}} \phi_{jm}. \tag{18, 19}$$

It will be noted that the quantity ϕ_{jm} is a function of α, j and m, only. It can easily be called by a computer algorithm.

With the values of A_m established as functions of the expansion coefficients E_j, the exact response of the first building block to a driving edge force distributed over the region $0 \leqslant \xi \leqslant \alpha$, and zero everywhere else, is known. It should be noted that even though one chooses a value k_L for the number of driving coefficients describing the driven edge force distribution (equation (14)) one need not restrict the number of terms k in the series describing the lateral displacement of the first and second building blocks (equation (2)) to this level. In fact it was found wise to choose k_L such that it is always greater than k divided by α. In this way the wave density in the response will be at least as high as the wave density in the distributed driving force. The second building block differs from the first only in that its driven edge is free of vertical edge reaction, but over the interval $0 \leqslant \xi \leqslant \alpha$ it is driven by a distributed bending moment. The bending moment distribution may be expressed as

$$\frac{M(\xi)b^2}{aD} = \sum_{j=0,1}^{k_L} F_j \cos\frac{j\pi\zeta}{\alpha}. \tag{20}$$

A solution for this second building block is obtained in terms of the driving coefficient F_j in a manner identical to that followed for the first building block.

The third building block is driven by a bending moment distributed all along the edge, $\eta = 1$. This edge is free of vertical edge reaction and the distribution of the moment amplitude is expressed in series form as

$$\frac{Mb^2}{aD} = \sum_{m=0,1}^{k} G_m \cos m\pi\xi. \tag{21}$$

It is very easy to obtain a solution for the response in terms of driving coefficients, G_m. The solution is taken in the form given by equation (2). The obtaining of solutions for this building block, and the next three building blocks is described in reference [1].

Solutions for the fourth, fifth and sixth building blocks are extracted from the above solution for the third building block. To extract a solution for the fifth building block one needs only replace the co-ordinate η of the above solution by the quantity $1 - \eta$. To extract the fourth building block solution from the third, one needs only interchange the co-ordinates ξ and η and replace the aspect ratio ϕ with its inverse. One must recall that the eigenvalue is still non-dimensionalized with respect to edge length a. Building blocks seven and eight are driven by concentrated harmonic forces of dimensionless amplitude P_1^* and P_2^*, and circular frequency ω at locations, $\xi = 0$, and $\xi = \alpha$, respectively, along their driven edges. These driven edges are also free of bending moment. Their solutions

are already available as they correspond to the intermediate solution obtained for the first building block.

Finally, one turns to the ninth building block. It has slip–shear conditions along all edges and is driven by a concentrated harmonic force of dimensionless amplitude P_3^* and circular frequency ω at co-ordinates u, v. A solution for this building block is obtained following established procedures. The block is divided into two segments as indicated in the figure. A solution for each segment is taken separately utilizing the co-ordinate systems shown. Both solutions are expressed in the form of equation (2). The concentrated force amplitude is represented by a Dirac function which in turn is expanded in a series identical to that of equation (2). Enforcing boundary conditions at $\eta = 0$, and conditions of continuity of displacement, slope, and bending moment, across the common segment boundary provides seven equations relating the eight unknowns. A final equation is based on equilibrium between the driving force and the vertical edge reactions of the two segments along their common boundary. One is thus able to express the response of the entire plate in terms of the amplitude of the harmonic driving force [2].

2.2. DEVELOPMENT OF EIGENVALUE MATRIX

An eigenvalue matrix is shown schematically in Figure 3. It corresponds to the type of matrix one would arrive at when utilizing three term expansions for the displacement of each building block (equation (2)), and applying for the present only one harmonic force at the support point. Several steps are required to arrive at this matrix. First, all nine building blocks are considered to be superimposed, one-upon-the-other. Since each term in each building block solution satisfies exactly the governing differential equation, the

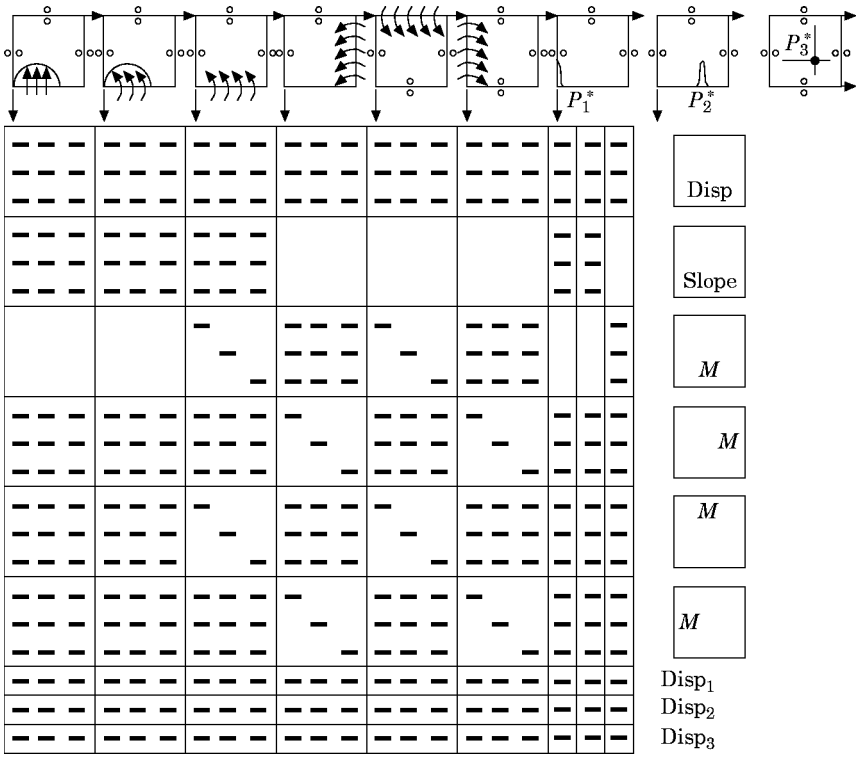

Figure 3. Schematic representation of eigenvalue matrix utilized in analysing partially clamped rectangular plate with single point support; displacements represented by three-term series.

combined set will also satisfy it. One needs only constrain the constants appearing in the combined solution so as to satisfy all prescribed boundary conditions.

The first step in setting up the eigenvalue matrix is to enforce the condition of zero lateral displacement along the edge, $\eta = 1$, in the region $0 \leqslant \xi \leqslant \alpha$. This is because α represents the extent of edge clamping. Toward this end one expands in a Fourier series, the contributions of all building blocks toward displacement in this region. A series of the type utilized in equation (14) was utilized here. One then demands that each net coefficient in this new series must equal zero. If k terms are utilized in the building block series solutions then k terms are utilized in this boundary series as well.

For illustrative purposes the matrix of Figure 3 was based on three-term expansions of the solutions. One therefore obtains three linear homogenous algebraic equations relating the unknown driving coefficients of the building blocks. This set of three equations is represented by the first three rows of the matrix of Figure 3.

Three more equations are obtained by enforcing the conditions of zero slope in the clamped region following identical steps. A further three equations are obtained by requiring that the contributions to bending moment along the edge, $\eta = 1$, of building blocks 3 through 9 must equal zero. Requirement that net contributions of all building blocks toward bending moments along the edges, $\xi = 1$, $\eta = 0$, and $\xi = 0$, must vanish, leads to nine further equations.

It is recognized that discontinuities in twisting moment at the extremities of the clamped region may lead to the existence of point forces at these extremities. For this reason building blocks seven and eight have been introduced. Two more equations are obtained when one requires that net displacement, at the point of application of the forces of these two building blocks, must vanish.

Finally, one turns to the ninth building block and requires that net displacement must equal zero at the co-ordinate u, v. The set of homogenous algebraic equation related to a partially clamped plate with one lateral point support was then described. The eigenvalue matrix for the problem is, in fact, the coefficient matrix for this set of equations. Eigenvalues are obtained by searching for those values of the parameter λ^2 for which the determinant of the eigenvalue matrix vanishes. Mode shapes are then obtained following standard procedures.

In the problem under study here one wishes to simulate the type of support the plate receives from a bolt with circular washer and cylindrical stand-off. Experience has shown that such support can be closely modelled by utilizing four discrete point supports of the type discussed above [2]. One point support is located at each extremity of two mutually perpendicular diameters running across the washer and parallel to one of the two plate edge directions. This is the manner in which bolt and stand-off support is modelled here.

3. COMPARISON OF COMPUTED AND EXPERIMENTAL RESULTS

The primary objective of the experimental work reported here is to verify the analysis presented above for the free vibration of partially clamped plates with, and without, rigid point supports.

3.1. PARTIALLY CLAMPED PLATES WITHOUT RIGID POINT SUPPORTS

It will be obvious that analytical studies of the free vibration frequencies and mode shapes for this family of plates can be conducted utilizing the building blocks of Figure 2 with building blocks related to rigid point support deleted. The last column of the eigenvalue matrix of Figure 3 will, of course, also be deleted. It will be appreciated that the analysis described here is not required in the classical case of a cantilever plate ($\alpha = 1$).

TABLE 1

Analytical and experimental resonant frequencies (Hz) *for partially clamped square plate* (10 × 10) (*experimental results in brackets*)

	α					
	0·25		0·50		0·75	
Mode number						
1	11·6	(10·8)	16·3	(15·7)	19·5	(18·9)
2	25·6	(24·7)	36·0	(35·0)	45·4	(41·8)
3	64·6	(63·6)	82·0	(81·2)	113·4	(106·8)
4	129·6	(127·9)	138·6	(137·0)	158·2	(155·8)
5	146·0	(145·8)	158·1	(157·9)	166·1	(161·2)
6	188·0	(183·7)	201·8	(199·1)	260·1	(253·4)

Eigenvalues for this classical problem are well known and tabulated in the literature [1]. The reader will find both experimental frequencies, and computed frequencies based on these classical eigenvalues of cantilever plates tabulated in the literature [3].

Experiments were conducted on two partially clamped aluminum plates of 10·0 in × 10·0 in (25·4 cm × 25·4 cm), and 10·0 in × 15·0 in (25·4 cm × 38·1 cm), respectively. Both plates were of 0·0615 in thickness (1·56 mm). Dimensionless clamping distances α were 0·25, 0·50 and 0·75. Resonant frequencies and the associated mode shapes for each plate were experimentally determined for the first six modes. The method of impact testing (roving hammer) was adopted. Only one accelerometer (type Endevco 2222C) was used; it was fixed at one suitable location, which was non-nodal for the first six modes. Since the weight of the accelerometer was only 0·5 g, the mass loading effect was negligible. The impact hammer was moved from one measurement point to another. Several measurement point locations were chosen in order to identify the mode shapes. For each point, a frequency–response function was obtained from the average of five impacts.

In Table 1 theoretical and experimental frequencies are presented for the first six modes of a partially clamped 10·0 in × 10·0 in aluminum plate. Values of α vary from 0·25 to 0·75 in intervals of 0·25. Experimental results are given in brackets. With the exception of the first mode frequency for the case $\alpha = 0{\cdot}25$, it is found that discrepancy between experiment and theory is equal or less than 3.5%. This is considered to constitute good agreement in tests of this type. It is found that all discrepancies are positive, i.e., the

TABLE 2

Analytical and experimental resonant frequencies (Hz) *for partially clamped rectangular plate* (10 × 15) (*experimental results in brackets*)

	α					
	0·25		0·50		0·75	
Mode number						
1	8·4	(8·2)	13·9	(13·4)	19·0	(18·6)
2	17·8	(17·6)	24·5	(23·6)	32·7	(32·6)
3	43·7	(41·4)	51·9	(49·1)	73·9	(78·0)
4	71·5	(71·2)	86·4	(83·5)	108·5	(105·7)
5	115·9	(114·8)	129·5	(130·4)	136·5	(136·7)
6	137·8	(136·6)	160·2	(156·2)	182·4	(183·9)

theoretical frequencies are slightly higher than those measured experimentally. It is known that when testing cantilevered plates experimentally, great caution must be taken to ensure that a truly clamped condition is achieved. Any deviation from this ideal condition will result in a slight lowering of measured frequencies. It is also known that measured plate vibration frequencies are very sensitive to variations in plate thickness and flatness.

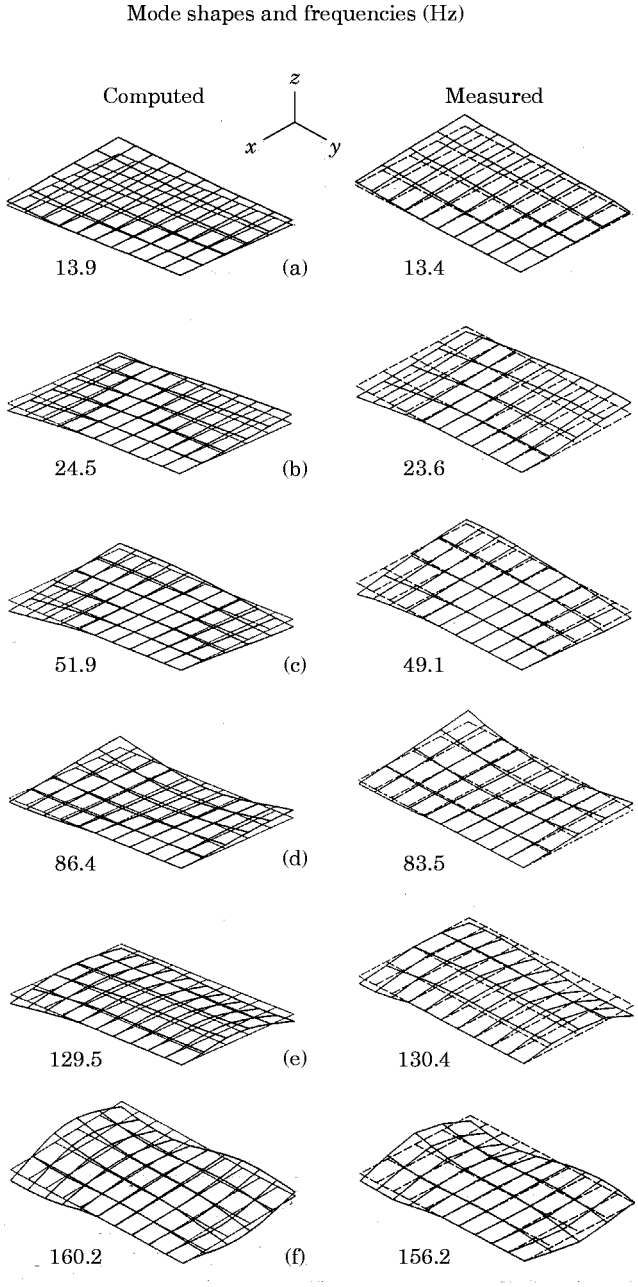

Figure 4. Computed and experimentally measured mode shapes for the first six modes of the plate of Table 2, with $\alpha = 0{\cdot}5$: (a) mode 1, (b) mode 2, (c) mode 3, (d) mode 4, (e) mode 5, and (f) mode 6.

TABLE 3

Analytical and experimental resonant frequencies (Hz) *for partially clamped* ($\alpha = 0{\cdot}75$) *rectangular plate* (10×15) *with rigid point support*

Mode Number	Analytical	Experimental
1	31·2	30·6
2	87·2	80·2
3	106·2	103·7
4	139·3	131·5
5	189·1	184·0

Furthermore, the actual plate properties; thickness, density, Young's modulus, and Poisson ratio, may differ slightly from those employed in the calculations.

In Table 2 theoretical and experimentally measured frequencies are presented for an aluminum plate similar to that to which the data of Table 1 pertains except that the plate is of dimensions 10·0 in × 15·0 in (25·4 cm × 38·1 cm) with partial clamping along the long edge. Both theoretical and experimental results are presented for the first six modes with α varying from 0·25 to 0·75 in intervals of 0·25.

It will be noted that agreement between theory and experiment is quite good. With the exception of the third mode the discrepancy between the two sets of results is generally within about 2.5%. Factors which can sometimes contribute to such discrepancies are difficulties in achieving idealized clamped conditions in the experimental set-up, as discussed earlier, as well as slight deviations from true isotropy in the rolled aluminum sheet. In both tables, as the parameter α increases the frequencies approach those of the fully clamped cantilever plate. The experimental results indicate that the analysis can be used with a high degree of confidence for design purposes.

Experimentally measured mode shapes for the first six modes of the plate of Table 2, with $\alpha = 0{\cdot}5$, are presented in Figure 4(a). The same family of mode shapes generated by the theoretical analysis are presented in Figure 4(b). A comparison of these two sets of mode shapes reveals a very good agreement. Ability to predict accurately these mode shapes is highly significant to circuit board designers who wish to locate electronic components in regions of low amplitude vibration. They will also wish to attach circuitry to regions of the board with low dynamic surface strain in order to avoid fatigue failure.

3.2. PARTIALLY CLAMPED PLATES WITH RIGID POINT SUPPORTS

Experimental tests were conducted on one partially clamped 10·0 in by 15·0 in aluminum plate of 0·0625 in thickness. The dimensionless clamping distance α was 0·75 along the long edge of the plate. Rigid point support was provided at co-ordinates, 13·7 in, 1·0 in

TABLE 4

Analytical and experimental resonant frequencies (Hz) *for partially clamped* ($\alpha = 0{\cdot}5$) *rectangular plate* (10×15) *with rigid point support*

Mode Number	Analytical	Experimental
1	30·15	28·5
2	54·7	52·8
3	84·9	80·4
4	134·2	128·0
5	176·6	171·1

($u = 13{\cdot}7/15{\cdot}0$, $v = 1{\cdot}0/10{\cdot}0$; Figure 1). In Table 3 theoretical and experimental frequencies are presented for the first five modes of the plate. It will be noted that fundamental mode theoretical and experimental frequencies are in very close agreement. Good agreement is also encountered for the higher modes where the difference between the theoretical and experimental frequencies is less than 5%. Results of a further theoretical and experimental study are presented in Table 4. These latter results differ from those of Table 3 only in that they were obtained with a value of $\alpha = 0{\cdot}5$. The agreement between experiment and theory is about equivalent to that encountered with the data of Table 3.

4. DISCUSSION AND CONCLUSIONS

The superposition method is found to be highly applicable for free vibration analysis of plates with the types of support discussed here. While the solutions should be of general interest it is known that they have application in the vibration analysis of electronic circuit boards. It will be obvious to the reader that the effects of any number of rigid point supports could be incorporated into the analysis. Each additional support will simply add four additional rows and columns to the eigenvalue matrix. There is no doubt that the analysis could be extended to handle problems with further complications. Examples of such problems would be those where elasticity is entered into the plate edge support [4]. Further complications that could easily be taken care of are the effects of local attached masses distributed over the plate surface. All of these problems are amenable to solution by following the mathematical procedure described here.

ACKNOWLEDGMENTS

This work was supported by a grant from the National Sciences and Engineering Research Council of Canada. Experimental work was carried out at the David Florida Laboratory of the Canadian Space Agency in Ottawa, Canada.

REFERENCES

1. D. J. Gorman 1982 *Free Vibration Analysis of Rectangular Plates*. New York: Elsevier-North Holland.
2. D. J. Gorman and R. K. Singal 1991 *American Institute of Aeronautics and Astronautics Journal* **29**, 838–844. Analytical and experimental study of vibrating rectangular plates on rigid point supports.
3. R. K. Singal, D. J. Gorman and S. A. Forgues 1992 *Experimental Mechanics* **32**, 21–23. A comprehensive analytical solution for free vibration of rectangular plates with classical edge conditions: experimental verification.
4. D. J. Gorman 1994 *Journal of Sound and Vibration* **174**, 451–459. A general solution for the free vibration of rectangular plates with arbitrarily distributed lateral and rotational elastic edge support.

APPENDIX: NOMENCLATURE

a,b	dimensions of plate
D	plate flexural rigidity
k_L	number of terms used in series representation of driving forces and moments in clamped region
k	number of terms utilized to represent Dirac function expansions and building block responses
M	amplitude of applied bending moment
Mb^2/aD	dimensionless bending moment

P	amplitude of concentrated force
P^*	dimensionless concentrated force amplitude $= -2Pb^3/Da^2$
u,v	spatial co-ordinates of concentrated forces divided by a and b, respectively
V	plate vertical edge reaction
Vb^3/aD	dimensionless vertical edge reaction
V_0	amplitude of dimensionless concentrated edge force
W	plate lateral displacement
ξ,η	distance in co-ordinate directions divided by a, and b, respectively
ζ	distance in co-ordinate direction divided by edge length a
α	length of edge clamping divided by edge length a
ϕ	plate aspect ratio $= b/a$
ω	circular frequency of plate vibration
ρ	mass of plate per unit area
λ^2	plate free vibration eigenvalue ($\omega a^2\sqrt{\rho/D}$)
ν	Poisson ratio
ν^*	$2 - \nu$